CHIN. PHYS. LETT. Vol. 35, No. 9 (2018) 098502

Temperature Dependence of Electrical Characteristics in Indium-Zinc-Oxide Thin Film Transistors from 10 K to 400 K *

Yuan Liu(刘远)[1,2,3], Li Wang(王黎)[2,3], Shu-Ting Cai(蔡述庭)[1**], Ya-Yi Chen(陈雅怡)[2,3], Rongsheng Chen(陈荣盛)[2,3], Xiao-Ming Xiong(熊晓明)[1], Kui-Wei Geng(耿魁伟)[2]

[1]*School of Automation, Guangdong University of Technology, Guangzhou 510006*
[2]*School of Electronic and Information Engineering, South China University of Technology, Guangzhou 510640*
[3]*Key Laboratory of Silicon Device Technology, Chinese Academy of Sciences, Beijing 100029*

(Received 14 June 2018)

The transfer characteristics of amorphous indium-zinc-oxide thin film transistors are measured in the temperature range of 10–400 K. The variation of electrical parameters (threshold voltage, field effect mobility, sub-threshold swing, and leakage current) with decreasing temperature are then extracted and analyzed. Moreover, the dominated carrier transport mechanisms at different temperature regions are investigated. The experimental data show that the carrier transport mechanism may change from trap-limited conduction to variable range hopping conduction at lower temperature. Moreover, the field effect mobilities are also extracted and simulated at various temperatures.

PACS: 85.30.Tv, 73.40.Qv, 73.50.Dn, 77.55.hf DOI: 10.1088/0256-307X/35/9/098502

Amorphous indium-zinc-oxide thin-film transistors (a-IZO TFTs) have drawn a great deal of attention in the flat panel displays and flexible electronics due to their excellent performance and good stability.[1] Moreover, IZO TFTs can be integrated with photodiodes to detect x-ray and cosmic rays.[2,3] Therefore, it can be used in some special applications, e.g., spacecraft, high-energy particle accelerators, and medical detectors. In these harsh environments, the devices may operate in a wide temperature range.[4,5] Thus the investigation of the temperature effect on IZO TFTs is urgently needed before they can be used in these special environments.

Temperature effects on conduction characteristics of oxide semiconductor devices have been reported by many groups.[6–13] The reduction of temperature may lead to the shift of threshold voltage, mobility, and sub-threshold swing.[6–8] Furthermore, the conduction mechanism may change from thermally activated band conduction to variable range hopping (VRH) in low temperatures.[9] However, these studies were only focused on the conduction performances in the normal operating temperature range. Up to date, variations of electrical characteristics of IZO TFTs in the range from helium temperature to extremely high temperature have been reported less.

In this Letter, the I–V characteristics of IZO TFTs are measured in the range of 10–400 K. The variations of threshold voltage ($V_{\rm th}$), field effect mobility ($\mu_{\rm FE}$), sub-threshold swing (SS), and leakage current ($I_{\rm leak}$) with temperature are extracted and discussed. Furthermore, the variations of the dominant conduction mechanism in the lower temperature are investigated. Thus the related shifts of field effect mobility with gate voltage are simulated at various temperatures.

The device used in this experiment was bottom gate structure IZO TFT with the channel width/length of 50 μm/10 μm. The lengths of gate/source and gate/drain overlap regions are about 1 μm. The thickness of the undoped IZO active layer was 30 nm. A 50-nm silicon oxide film with 250-nm silicon nitride film was used as the gate dielectric. The measured gate insulator capacitance per unit area was about 13.6 nF/cm^2. A detailed description of the processing steps was provided elsewhere.[14] The I–V measurements were performed by an Agilent B1500. The device was mounted on the sample holder of a variable temperature helium cryostat (Janis CCS-450).

The transfer characteristics of IZO TFTs were measured at various temperatures, ranging from 10 to 400 K, as plotted in Fig. 1. With the increment of temperature, negative shifts of transfer curves have been observed while the leakage current increases above 340 K. The extracted threshold voltage, field effect mobility, sub-threshold swing, and leakage current at various temperatures are shown in Fig. 2.

Using the linear extrapolation method, threshold voltages were extracted from the transfer curves when $V_{\rm ds} = 0.1$ V.[15] Generally, the extracted threshold voltage is a strong function of the density of point defects, which involves deep donor-like states and shallow donor-like states.[10,16] As plotted in Fig. 2(a), the negative shifts of $V_{\rm th}$ in the range of 10–300 K are induced by the deep donor-like states, which refer to oxygen vacancies in amorphous oxides.[10,16] Above 300 K, the shift of $V_{\rm th}$ may be caused by the hydrogen which is emitted from the passivation layer (PECVD-

*Supported by the National Natural Science Foundation of China under Grant No 61574048, the Pearl River S&T Nova Program of Guangzhou under Grant No 201710010172, the International Science and Technology Cooperation Program of Guangzhou under Grant No 201807010006, and the Opening Fund of Key Laboratory of Silicon Device Technology under Grant No KLSDTJJ2018-6.
**Corresponding author. Email: shutingcai@gdut.edu.cn
© 2018 Chinese Physical Society and IOP Publishing Ltd

SiO_2 film) and thus absorbed by the IZO film.[10,11]

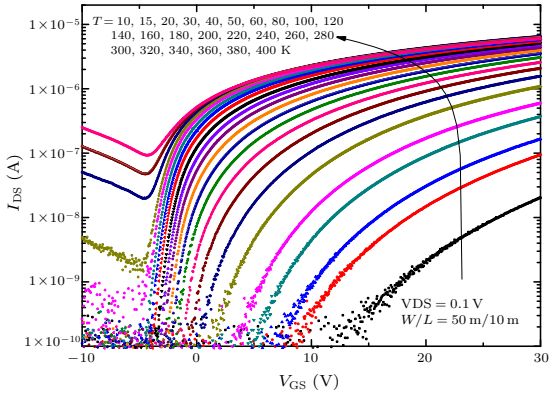

Fig. 1. Transfer characteristics of IZO TFTs measured at various temperatures.

The field effect mobilities are extracted from measured transconductance (g_m) when $V_{gs} - V_{th} = 10$ V and $V_{ds} = 0.1$ V, which are dominated by the percolation conduction mechanism under this condition. As plotted in Fig. 2(b), the extracted field effect mobility firstly increases from 0.23 to 33.2 cm^2/Vs with increasing temperature, and then decreases to 30.2 cm^2/Vs at 400 K. The shifts of field effect mobility may be governed by two different mechanisms. In the range of 10–360 K, the carrier transport is dominated by multiple trapping and release events.[8] As reported previously,[17,18] most of the charges induced in the channel of IZO TFTs are trapped in the localized states and only a small fraction of charges are free carriers. Therefore, the field effect mobility can be expressed by $\mu_{FE} = \mu_{band} Q_{free}/Q_{tot}$, where μ_{band} is the band mobility, Q_{free} is the amount of free carriers, which can be expressed as $Q_{free} = N_C \exp[(E_F - E_C)/kT]$, and Q_{tot} is the total charge induced in the channel, which can be calculated by $Q_{tot} = C_{ox}(V_{gs} - V_{th})$. Based on these equations, the field effect mobility is strongly dependent on the amount of free carriers. With the increment of temperature, Q_{free} increases sharply and thus induces to the increment of the extracted mobility. Moreover, the relationship between mobility and temperature is an exponential function and can be expressed by $\mu = \mu_0 \cdot \exp(-E_D/kT)$, where μ_0 is the mobility prefactor (about 47.1 cm^2/Vs in this work), and E_D is the electron mobility activation energy (about 14.1 meV). Above 360 K, the Fermi level reaches the degenerate like states, which causes the scattering mean free path to be greatly reduced by the thermal effect.[19] Thus the extracted field effect mobility may decrease with increasing temperature.

The sub-threshold swing is defined as the reciprocal of the slope of the $\log(I_{ds}) - V_{gs}$ curve in the sub-threshold region.[15] As plotted in Fig. 2(c), the extracted sub-threshold swings were negligibly changed in the range of 100–300 K, which indicates that the densities of localized states were not changed in the active layer. The increment of SS above 340 K may be induced by the generation of shallow donor-like states, which are caused by the hydrogen emitted from the passivation layer.[10,12] In addition, the increment of SS with decreasing temperature below 100 K may be induced by the transition of the conduction mechanism, which will be discussed in the following.

The leakage currents are extracted when $V_{gs} = -5$ V at various temperatures. As shown in Fig. 2(d), significant increments of leakage currents have been observed above 340 K, which may be related to the back channel leakage currents.[20] As reported previously,[20] the notable increase of leakage current with temperature may occur when the active layer is thick enough and thus the full depletion region may not cover in the whole active layer. The density of free carriers located near the back IZO/passivation interface may increase and thus a notable parallel current may exist with increasing temperature. This phenomenon may induce the increment of leakage current, and thus the drain current will be out of gate control.

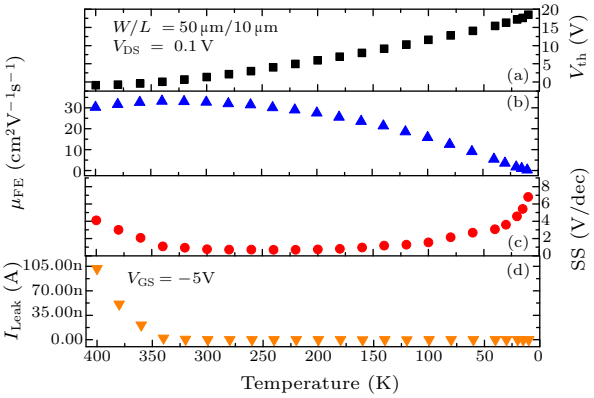

Fig. 2. Temperature dependence of electrical parameters: (a) V_{th}, (b) μ_{FE}, (c) SS, and (d) I_{leak}.

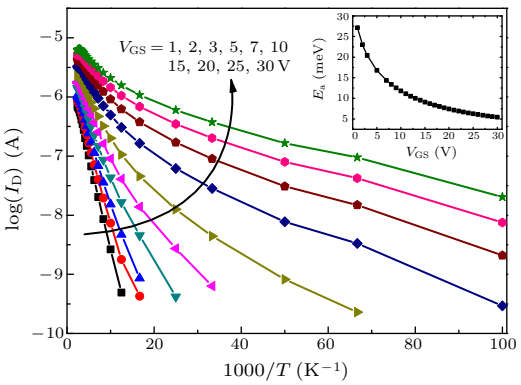

Fig. 3. Drain current I_{DS} versus $1000/T$ at various V_{GS}.

As discussed above, the drain current is highly dependent on the ambient temperature, thus the carrier transport mechanism of IZO TFTs at various temperatures should be further investigated. The temperature dependences of the drain current (I_{ds} versus $1000/T$) at various gate voltages are shown in Fig. 3. In the temperature range of 100–400 K, the drain current can

be well fitted to the Arrhenius equation[9,21]

$$I_{\rm DS} = I_{\rm DS0} \cdot \exp(-E_{\rm a}/kT), \tag{1}$$

where $I_{\rm DS0}$ is a prefactor of drain current, and $E_{\rm a}$ is the activation energy.

In amorphous oxide semiconductors, the linear relationship between $I_{\rm DS}$ and $1000/T$ in a semilogarithmic plot represents that the trap-limited conduction (TLC) is the dominant carrier conduction mechanism.[6,22] Based on the TLC model, the charge transport occurs through the delocalized band and the trapped carriers in the localized states must be thermally excited into the band to contribute to the charge transport. With increasing temperature, the trapped carriers are more easily excited to the delocalized states and thus lead to more free carriers in the conduction band. Therefore, the on-currents in the IZO TFTs are thermally activated and obey the Meyer–Neldel rule.

The variation of extracted $E_{\rm a}$ with gate voltage is plotted in the inset of Fig. 3. It is well known that most of the induced charges in the channel are captured by localized states with a small fraction going into the conduction band.[9,12] With increasing gate voltage, the extracted $E_{\rm a}$ decreases and the Fermi level moves towards the conduction band edge. The movement of the Fermi level is determined by the distribution of localized states. Generally, the extracted $E_{\rm a}$ in the IZO TFTs are much lower than that in the a-Si:H TFTs, which is ascribed to a much steeper distribution of localized states for the bulk IZO layer than that for the bulk a-Si:H layer.[12]

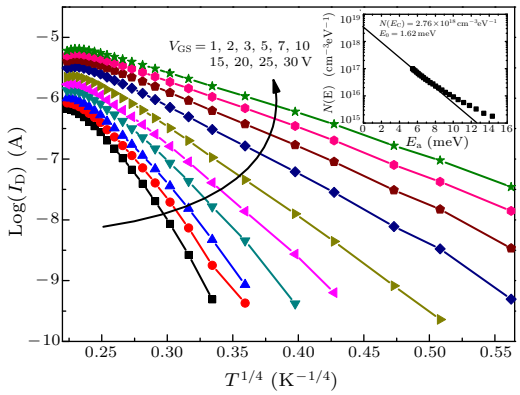

Fig. 4. Drain current $I_{\rm DS}$ versus $T^{-1/4}$ at various $V_{\rm GS}$.

The measured currents deviate from the Arrhenius equation when the temperature is below 100 K, which indicates that TLC is no longer the dominant mechanism in the sub-threshold and transition regions.[9] As shown in Fig. 4, $\log(I_{\rm ds})$ may linearly decrease with $T^{-1/4}$ below 100 K. These data indicate that VRH may be the dominant mechanism and the currents can be fitted by Mott's equation below 100 K,[9]

$$I_{\rm DS} = I_{\rm DSV} \cdot \exp(-B/T^{1/4}), \tag{2}$$

where $I_{\rm DSV}$ is the drain current prefactor for variable range hopping, B depends on the material properties which can be calculated by $B = 2(\alpha^3/kN(E))^{1/4}$, α is the reciprocal of the Bohr radius (about 1.79 nm), and $N(E)$ is the density of states at Fermi level.

Based on Eq. (2), $N(E)$ can be extracted. Combining with the extracted activation energy, the distribution of $N(E)$ in the band-gap can be plotted, as shown in the inset of Fig. 4. The extracted data can be fitted to $N(E) = N(E_{\rm C})\exp(-E_{\rm at}/E_0)$, while $N(E_{\rm C})$ is about 2.76×10^{18} cm^{-3}eV^{-1} and E_0 is about 1.62 meV. These extracted data are similar to the reported values.[6]

According to Mott's VRH theory, a hopping electron will always try to find the lowest activation energy and the shortest hopping distance.[23] The hopping distance may increase with the decrement of temperature. Therefore, more localized states may exist in a longer conduction path with a lower barrier potential. Thus the related concentration of localized states may increase, leading to the increment of extracted SS in the lower temperature, as shown in Fig. 2(c).

As discussed above, the dominant conduction mechanism may change from TLC to VRH with decreasing temperature. Thus the field effect mobility in the IZO TFTs at various temperatures can be simulated. The field effect mobility can be retrieved from the transconductance in the deep linear region[15,24]

$$\mu_{\rm FE} = \frac{\partial I_{\rm DS}}{\partial V_{\rm GS}} \frac{1}{C_{\rm ox}(W/L)V_{\rm DS}}. \tag{3}$$

At high temperatures, carriers are thermally emitted and the transport mechanism may be dominated by TLC. Thus the field effect mobility in the above threshold region can be fitted by[25]

$$\mu_{\rm FE} = \mu_{\rm b}^* A^* (V_{\rm GS} - V_{\rm th})^{2(T_{\rm t}/T-1)}, \tag{4}$$

where $\mu_{\rm b}$ is the band mobility, $T_{\rm t}$ is the characteristic temperature of tail states (about 315 K in room temperature), and A^* is a fitting parameter related to the concentration of tail states.

At lower temperature, the thermal activation energy is insufficient to release electrons into the conduction band, and the transport mechanism may be dominated by VRH. Thus the field effect mobility in the above threshold region can be fitted by[25]

$$\mu_{\rm FE} = \mu_0^* B^* \exp(-(T_0/T)^{1/4})(V_{\rm GS} - V_{\rm th})^{\alpha}, \tag{5}$$

where μ_0 is the hopping conduction mobility, T_0 is the characteristic temperature of localized states (about 10^8 K), B^* is a fitting parameter related to the density of localized states, and α is about 0.4 at 80 K.

The extracted mobility and simulated mobility are shown in Fig. 5. Good agreements are achieved between extracted data and simulated data in the above-threshold region. In addition, the deviation observed under the higher $V_{\rm GS}$ conditions above 120 K may be related to another change of conduction mechanism. As reported,[10,25,26] the carrier transport mechanism

in the oxide TFTs may change to percolation conduction at high gate voltages.

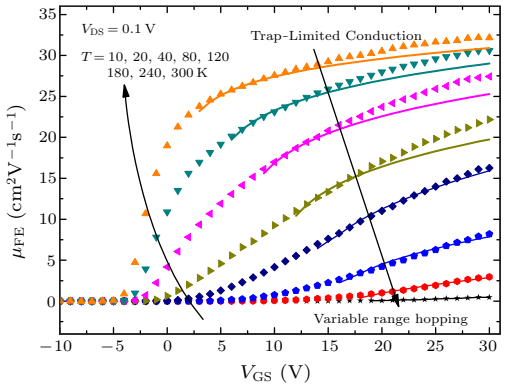

Fig. 5. Extracted (dots) and simulated (lines) field-effect mobility at various temperatures.

In summary, temperature effects in the IZO TFTs have been studied in the range of 10–400 K. The influences of temperature on threshold voltage, subthreshold swing, field effect mobility, and leakage current are analyzed. Furthermore, the transition of the transport mechanism of IZO TFTs are discussed. The dominated carrier transport mechanism may change from trap-limited conduction to variable range hopping conduction below 80 K. Moreover, the field effect mobilities at various temperatures are extracted and simulated.

References

[1] Lan L, Xiong N, Xiao P et al 2013 *Appl. Phys. Lett.* **102** 242102
[2] Cramer T, Sacchetti A, Lobato M T et al 2016 *Adv. Electron. Mater.* **2** 1500489
[3] Gelinck G H, Kumar A, Moet D et al 2016 *IEEE Trans. Electron Devices* **63** 197
[4] Ramirez J I, Li Y Y V, Basantani H et al 2015 *IEEE Trans. Nucl. Sci.* **62** 1399
[5] Liu Y, Wu W J, En Y F et al 2014 *IEEE Electron Device Lett.* **35** 369
[6] Kim H J, Hong S Y, Kim D H et al 2017 *J. Vac. Sci. Technol.* B **35** 030602
[7] Heo K, Cho K S, Choi J Y et al 2017 *IEEE Trans. Electron Devices* **64** 3183
[8] Liu Y, Wu W J, Qiang L et al 2015 *Chin. Phys. Lett.* **32** 088506
[9] Chowdhury M D H, Migliorato P and Jang J 2013 *Appl. Phys. Lett.* **103** 152103
[10] Godo H, Kawae D, Yoshitomi S et al 2010 *Jpn. J. Appl. Phys.* **49** 03CB04
[11] Jeong J, Lee G J, Kim J et al 2013 *J. Appl. Phys.* **114** 094502
[12] Takechi K, Nakata M, Eguchi T et al 2009 *Jpn. J. Appl. Phys.* **48** 011301
[13] Hoshino K and Wager J F et al 2010 *IEEE Trans. Electron Devices* **31** 818
[14] Liu Y, Chen R S, Li B et al 2018 *IEEE Trans. Electron Devices* **65** 356
[15] Arora N 2007 *MOSFET Modeling for VLSI Simulation: Theory and Practice* (Singapore: World Scientific)
[16] Wang L, Liu Y, Geng K W et al 2018 *Chin. Phys.* B **27** 068504
[17] Shur M and Hack M 1984 *J. Appl. Phys.* **55** 3831
[18] Liu Y, Yao R H, Li B et al 2008 *IEEE/OSA J. Disp. Technol.* **4** 180
[19] Chen B Y, Wu W H and Chen J R 1995 *J. Mater. Sci.* **30** 2254
[20] Estrada M, Rivas M, Garduno I et al 2016 *Microelectron. Reliab.* **56** 29
[21] Chen C, Abe K, Humomi H et al 2009 *IEEE Trans. Electron Devices* **56** 1177
[22] Guo D, Miyadera T, Ikeda S et al 2007 *J. Appl. Phys.* **102** 023706
[23] Kamiya T, Nomura K and Hosono H 2009 *J. Disp. Technol.* **5** 462
[24] Jeong J, Lee G J, Kim J et al 2012 *J. Phys.* D **45** 135103
[25] Lee S, Nathan A, Robertson J et al 2011 *Technical Digest-International Electron Devices Meeting* **343** 14.6.1
[26] Torricelli F, Meijboom J R, Smits E et al 2011 *IEEE Trans. Electron Devices* **56** 2610